Comparison and optimization of five desalination systems on the inner walls of Saint Philibert Church in Dijon, France

Ann Bourgès [1], Véronique Vergès-Belmin [2],

[1] Dr, Cercle des Partenaires du Patrimoine, Champs sur Marne, France
"ann.bourges@culture.gouv.fr"
[2] Dr, Laboratoire de Recherche des Monuments Historiques, Champs sur Marne, France « veronique.verges-belmin@culture.gouv.fr »

Abstract

In the framework of the European project "Desalination", the Saint Philibert site has been selected as a field study to assess and compare the effectiveness of five desalination poultices after one application. These poultices were applied on two inner walls on the south side of the church. The decrease of salt concentration as well as the depth of desalination was taken into consideration in the definition of the effectiveness. This paper strongly underlines the close link between the effectiveness of desalination treatments and the properties of both stone and poultice materials. Analyses suggest that pore size distribution of the poultices should overlap pore size of the substrate for optimization of desalination efficiency. Moreover, size and arrangement of grains are probably important parameters to take into consideration when formulating poultices, as they directly influence the capillary suction of the solubilized salt solution.

Keywords

Desalination, poultice, pore size distribution.

Introduction

Practitioners and scientists have studied various ways to remove salts from a substrate and elaborated desalination methods [Vergès-Belmin and Siedel, 2005]. Desalination through poultices is one of these methods. A poultice is made of one or several hydrophilic moistened materials and applied on the object. The water penetrates from the poultice into the porous space and dissolves the soluble salts. The evaporation of water from the poultice and the capillary transport from the substrate to the poultice should lead to salt extraction. Optimal efficiency in salt solution removal is theoretically achieved if the pores of the wet poultice are finer than those of the substrate, thus allowing the poultice to exert capillary suction forces on the substrate

[Terheiden et al, 2002]. If such a model did work, it would be possible to tailor the pore size and distribution of the poultice to that of the substrate. However, many other parameters may influence desalination efficiency, one of them being the poultice adhesion to the substrate. In order to better understand the desalination process, our team has studied different kinds of poultices, first in the laboratory (reference) and then on site, where a selection of five desalination systems was applied. This paper reports on the results of this study, with an emphasis on the relationships between stone and poultice's physical properties.

1. Preliminary investigations and test set up

1.1. The site and its building stone

The selected site was Saint Philibert Church in Dijon (France). Built with dense limestone in the XIIth century, the building has been used since the French Revolution as a salt storage place. In 1972, a concrete plate was installed for the purpose of ground heating. The soil, already loaded with sodium chloride, could only evaporate through the masonry. Rapid and severe decay occurred until the weakness of the structure forbade any public access to the site.

The limestone of Saint Philibert Church is characterized by a very low total porosity (5.7 %) and a low water uptake coefficient (1.1 kg/m^2/h$^{0.5}$). Pore size distribution of the stone is unimodal, spread from 0.01 µm to 0.1 µm, but mainly centered on 0.03µm.

1.2. Condition mapping

Two specific walls were selected to be desalinated, the walls named S6 and S7. The criteria for such a selection were the presence of a homogeneous distribution of both lithotype and mortar on the one hand, and alteration patterns on the other hand. Three decay zones were observed (see Figure 1): at the bottom of the wall (up to 100cm height) a white veil is identified, then in the middle part of the wall (150cm) salt efflorescence and encrustation can be seen, and finally, in the higher level between 200cm and 250cm, severe scaling is taking place, leading to back weathering, hard pointing mortars being left unaltered and prominent.

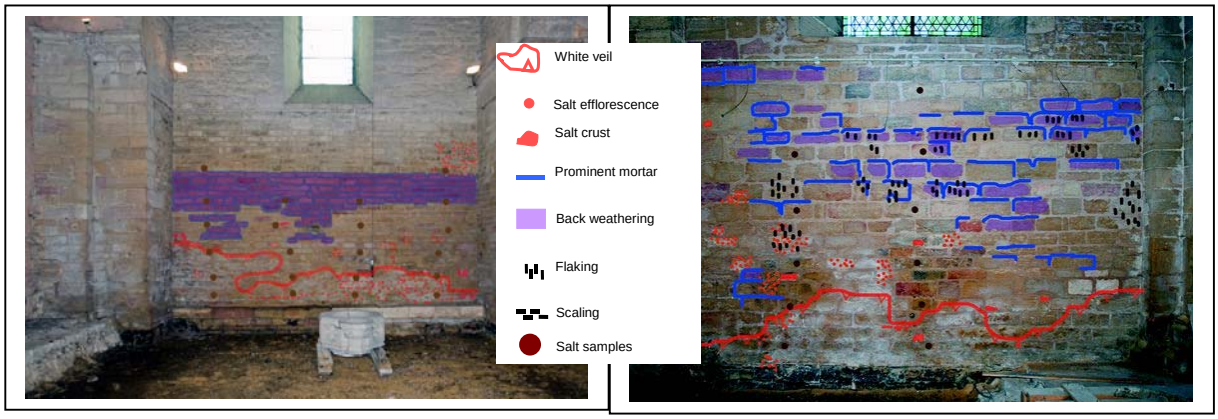

Figure 1. Condition mapping of the two selected walls S7 and S6 in St Philibert Church.

1.3. Nature of salts

Samples of efflorescence and crust were taken from the surface of the two selected walls in order to identify the crystallized phases by X ray diffraction (Diffractometer Bruker D8 Advance). Powder samples were collected by drilling the stones, and the soluble salt content was quantified with ion-chromatography (IC), using an I.C. Dionex DX320, with pump-detector IC25, automatic injector AS50 and thermostatic columns AS50. Sample solubilization followed the Italian standard 13/83 [Normal, 1983]. Analysis by Xray diffraction (XRD) identified the presence of low soluble salts (gypsum), fairly soluble salts (trona) and more soluble salts (thenardite and halite). Calcite, often identified with these salts, probably came from stone disintegration.

1.4. Salt quantification and distribution

Drilling powder samples were collected on each area where a poultice was to be applied. They were taken at different depths (0-0.5 / 0.5-1 / 1-2 / 2-3.5 / 10-20cm), with an electrical drilling device fitted with a 0.8 cm diameter bit, and along vertical transepts at the following heights: 50, 92, 138, 188, 248 and 308 cm for the wall S6, and 93, 133, 183, 239, 289, 349 cm for the wall S7.

The nature and distribution of soluble salts is clearly linked to the distribution of decay patterns (see Figures 1 and 2). Indeed, with IC we could identify sodium and chloride at higher levels, where scaling and back weathering were observed. These ions were more concentrated at the surface but were mostly detected up to a depth of 20cm (see Figure 2). They are most probably associated as halite (NaCl), this salt being the one reported as the major contaminant of the walls in historical records. Potassium, associated with nitrates (nitre), is present in the same level as sodium chloride and shows the same concentration pattern. It is most probable that the intense scaling on the higher part of the investigated walls is mostly due to halite, and to a minor extent, also to nitre crystallization.

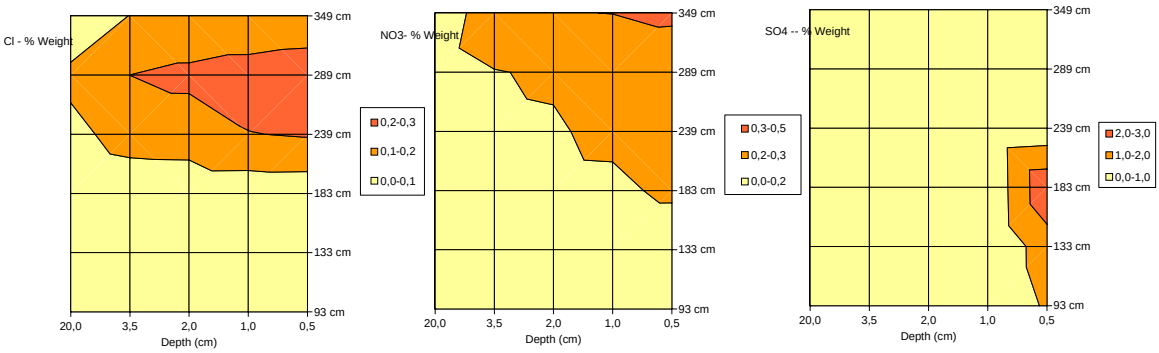

Figure 2. Concentration of Cl^-, NO_3^-, SO_4^{--} in weight % as a function of depth and height on the wall S7.

Calcium, clearly linked to sulphates, is identified on the lower part of both walls (S6: 93-235cm; S7: 50cm-308cm). These ions are exclusively concentrated near the surface, up to a depth of 1cm, and correspond to gypsum ($CaSO_4.2H_2O$) identified by XRD. Their location indicates that they most probably form the white veil mentioned

before. Salt analyses show that both walls S6 and S7 are contaminated with identical salts, which are distributed in the same way, and have a similar concentration.

1.5. Selection, characterization and application of poultices

A specific methodology was used to select poultice recipes to be applied in Saint Philibert. First, a large list of recipes was compiled on the basis of a response by users to an enquiry in Europe, and from the extensive literature on the topic [Bourgès and Vergès-Belmin, 2008]. Eleven poultices were tested in the laboratory and five of them were finally selected on the basis of workability, adhesion and shrinkage tests: a pure cellulose powder mixture (P1) (BC1000/BW40, respectively 700 and 200 µm fibre length); two clay-based poultices – kaolin/sand (P2) and bentonite/sand (P3); a mixture of cellulose BW40, kaolin and sand (P4); and finally, one based on fine quartz sand (~ 200 µm) mixed with fume silica (P5). Material specifications: BC 1000 and BW40 are from Arbocel®; Kaolin: IMERYS quality China Clay Speswhite Powder; Bentonite quality Impersolt: Société Française des Bentonites et des Argiles; CEN196 Sand fraction sieved at 0.5-1 mm. Table 1 presents the main properties of the selected poultices.

	Ratio dry powder in vol	Volume of water	Ratio dry powder in weight	Wc	l/m^2	kg/m^2 (dry material)
BC 1000/BW40	1 :1	1.4	1:2.1	4.5	9.8	2.2
Kaolin/sand	0.8 :1	0.4	1:5	0.2	3.6	18.4
Bentonite/sand	1 :2	1.5	1:6	0.33	5.2	15.8
BW40/kaolin/sand	1 :0.8 :1	0.9	0.5:1:4.5	0.4	5.6	13.9
Fine sand/fume silica				0.35	6.2	18.3

Table 1. Main properties of five the selected poultices. Wc corresponds to the ratio of water to the dry powder, l/m^2 is the quantity of water used per square meter, kg/m^2 is the quantity of dry material used per square meter.

Among these recipes, the cellulose poultice shows the highest linear shrinkage (9%), partly because it is also the highest water absorbing material (10 l/m^2). Mixtures containing clay minerals, kaolin/sand, BW40/kaolin/sand and bentonite/sand show a moderate shrinkage (respectively 1%, 5% and 4 %), and finally the fine sand mixed with fume silica has a negligible dimensional change after drying (0.5%).

Poultices recipes were prepared the day before application. Before poultice application, the surface of the walls was brushed to remove loose stone particles and stone dust. Each application area measured 280 cm in height by 70 cm in width and was delimited by wooden laths. Climatic conditions during application varied between 10 and 12°C and between 65 and 70 RH %. A team of conservators applied the poultices manually. The poultices remained on the walls for 5 months, until they totally dried.

2. Results and discussion

2.1. Observations after application and after drying

Forty-eight hours after application, a network of cracks appeared on some of the poultices. Bentonite/sand poultice showed this feature. No detachment could be noticed after two days, but after the entire drying period was completed more than 50 % of the poultice was detached. A curling phenomenon was observed, suggesting that the substrate dried before the poultice – the humidity gradient being too different between the poultice and the substrate. Large cracks were also observed on BC1000/BW40 and BW40/kaolin/sand poultices (see Figure 3). They led to early detachment, only after two days, especially on the upper level of the poultice. Water seeped from the top to the bottom of BC1000/BW40 poultice, leading to a faster drying on its upper part. More than 50 % of the BC1000/BW40 poultice was detached after drying entirely, while the detachment of the BW40/kaolin/sand poultice was localized around the initial cracks formed at forty-eight hours. Moreover poultice pieces had a good adhesion to the substrate. Only the kaolin/sand and fine sand/fume silica poultice did not show any detachment from the substrate, even when totally dry.

Figure 3. Location of the five poultices, and detachment areas after dryng. From left to right: BC1000/BW40 (P1); kaolin/sand (P2); bentonite/sand (P3); BW40/kaolin/sand (P4) and fine sand/fume silica (P5).

2.2. Efficiency

Desalination efficiency can be evaluated in many ways. As we had tested some of the poultice recipes evaluated by Domaslowski in his 1998 publication, we considered using the same evaluation procedure as the one he proposed. It consists of calculating the quantity of salts extracted versus the quantity of salts originally present in the contaminated substrate. Domaslowski (1998) did not indicate the type of ions extracted but considered all salts in a general manner. In our case, the calculation was made for each ion (Cl^-, $NO3^-$, $SO4^{--}$), taking into consideration the entire batch of samples, i.e. the five heights and the four depths, except sulphates, for which only the two first depths (0-0.5 and 0.5-10 mm) were considered (see Figure 4). The results obtained at St Philibert are similar to those of Domaslowski (see Figure 4). Indeed, mixtures containing kaolin show the best results with an extraction above 50% and in the same range for chlorides and nitrates. BW40/kaolin/sand also showed a good performance, despite of the cracks observed on the poultice. In contrast, bentonite/sand poultice shows much lower efficiency (10%) than expected from Domaslowski results, probably because it detached during drying. The cellulose poultice (BW40/BC1000) did not extract any salt, while Domaslowski (1998) showed an efficiency of 50% for cellulose-based poultice. The only poultice recipe not investigated before (fine sand/fume silica) showed a poor efficiency (10%). It presents a remarkably better result for nitrates than for chlorides. As far as sulphates are concerned, they could hardly be extracted by any of the poultices, only kaolin/sand poultice revealed a low efficiency.

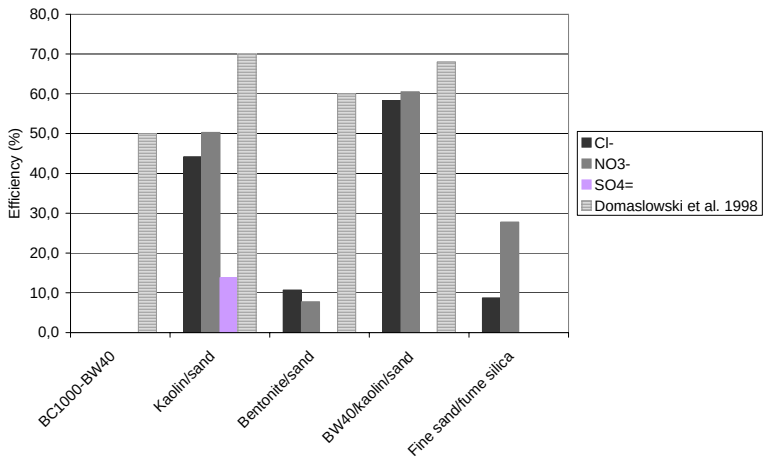

Figure 4. Influence of poultice type on desalination efficiency.

Let us consider now the way the salts are distributed along the four sampling depths at the upper part of the vertical profiles after desalination. Figure 5 illustrates desalination profiles of the two kaolin bearing poultices, kaolin/sand (P2) and BW40/kaolin/sand (P4). The plain line represents the chlorides concentration in weight % before desalination and the dash line after desalination. Both poultices do extract salts, but the profiles have different shapes. Indeed, kaolin/sand poultice presents an even extraction profile, while BW40/kaolin/sand poultice reveals an important decrease of chloride concentration in depth, but a concentration close to the surface. The average extraction is better but salts are accumulated close to the surface.

A similar consideration can be applied to the bentonite/sand (P3) and fine sand/fume silica (P5) poultices, for which an extraction is noted along the entire profile (up to a depth of 3.5 cm), but a salt accumulation is present close to the surface and at a higher level than before desalination (see Figure 5). For these two poultices, salts have moved toward the surface, but could not be absorbed by the poultice. In this case there is a problem at the interface between the poultice and the substrate; the suction of the poultice is not strong or long enough to get all the salts out of the substrate. It can be noticed that the bentonite/sand poultice was found to be detached after it had totally dried. In this case, the poultice detached during the slow drying of the substrate and the salt solution was carried to the surface.

In the case of the cellulose poultice BW40/BC1000 (P1), a higher Cl^- concentration was observed along the whole depth (see Figure 5). The high quantity of water brought by this poultice seems to have carried salts that were distributed more deeply towards more superficial layers. As it was underlined by the analysis before desalination, chloride and nitrate are present deep within the wall and are thus an important source of salts. Furthermore, as observed before, once the poultice is detached, the substrate continues to dry naturally carrying the salts in solution to the evaporation front, i.e. to the surface

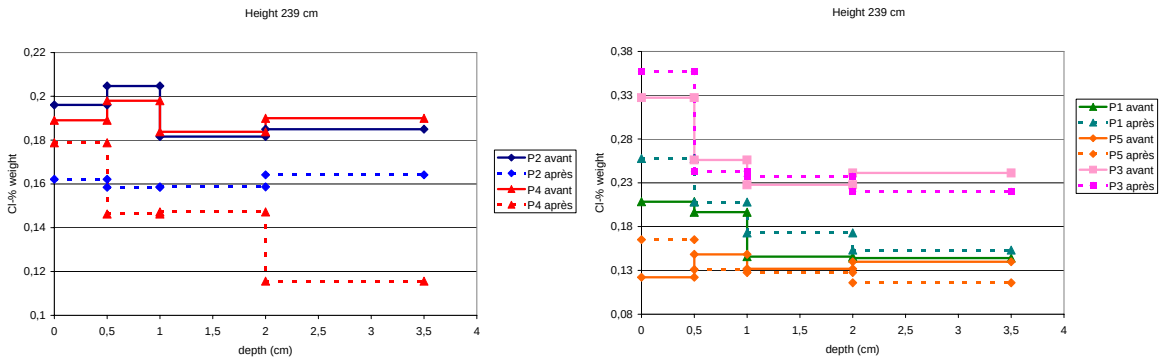

Figure 5. Concentration profiles of Cl^- in the stone for different poultice recipes before and after desalination. Left chart: P2 (Kaolin/sand) and P4 (BW40/kaolin/sand). Right chart: P1 (BC1000/BW40), P5 (Fine sand/fume silica) and P3 (Bentonite/sand).

2.3. Microstructural characteristics of poultices and substrate: an interpretation

Both theoretically and for optimized desalination, the suction forces of the poultice should be higher than the suction forces of the substrate to allow ions in solution to be driven toward the poultice. Thus, the determination of pore size can be of much help to understand poultice behaviour on a specific substrate. We performed such measurements on both substrate and poultices (see Figure 6). We assume here that the pore structures of the poultice measured and observed in a dry state are very close to that of the poultice when suction is operating from the substrate. Indeed, our lab experiments proved that shrinkage starts to appear as soon as the poultice is applied and reaches more than 50% of its final value after 48h, the extraction of salts in solution apparently beginning later on, and lasting up to two weeks. Figure 6 clearly

shows that the curve of the substrate overlaps that of the kaolin/sand and BW40/kaolin/sand poultice

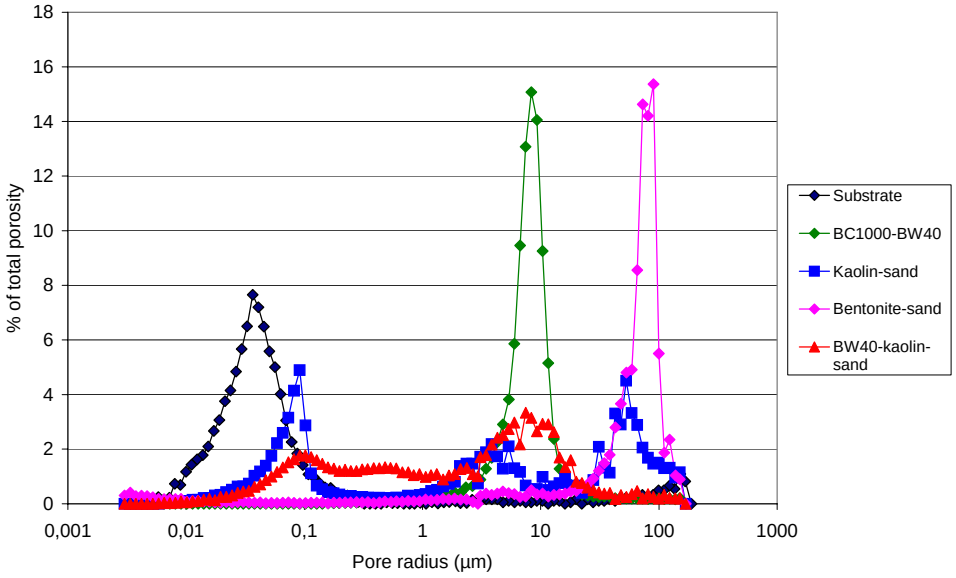

Figure 6. Pore size distribution of the substrate and the poultices.

The kaolin/sand poultice presented a diversified pore size distribution. Three pore sizes can be observed by mercury intrusion porosimetry (MIP) and are confirmed by scanning electron microscopy (SEM) (see Figures 6 and 7). The peak centred on 90 µm corresponds to a part of the intergranular pores between sand grains, the peak around 10 µm relates to the connection between clay binder and sand grains, and the 0.03-0.1 µm peak corresponds to the pore space between clay platelets. Kaolin coats the sand grains evenly; kaolinite platelets are well identified and form an unsorted system where pores are open and interconnected.

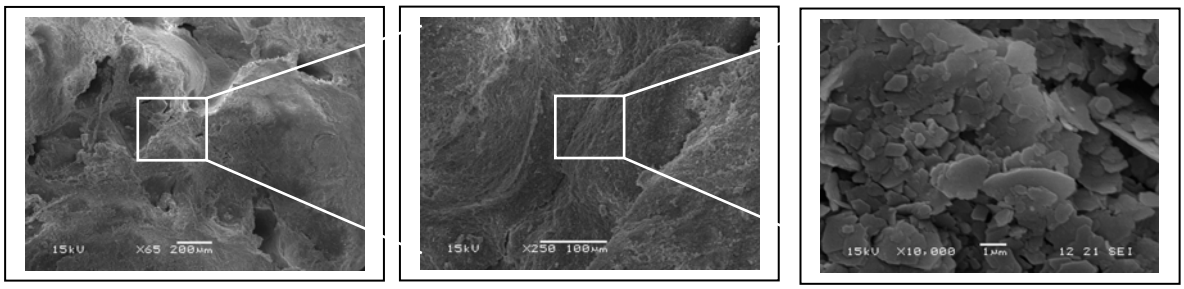

Figure 7. Secondary electron images of the kaolin/sand poultice at three different scales.

Similar considerations can be addressed to the BW40/kaolin/sand poultice, which shows pores in the range 0.003-0.1 µm, corresponding the arrangement of kaolin platelets (see Figures 6 and 8). Nevertheless, pore size distribution of this mixture is more regularly distributed and shows a real range of pores from 0.003 to 10 µm. The pore space between sand grains is probably filled by the cellulose, while kaolin creates a heterogeneous coating of the cellulose fibres.

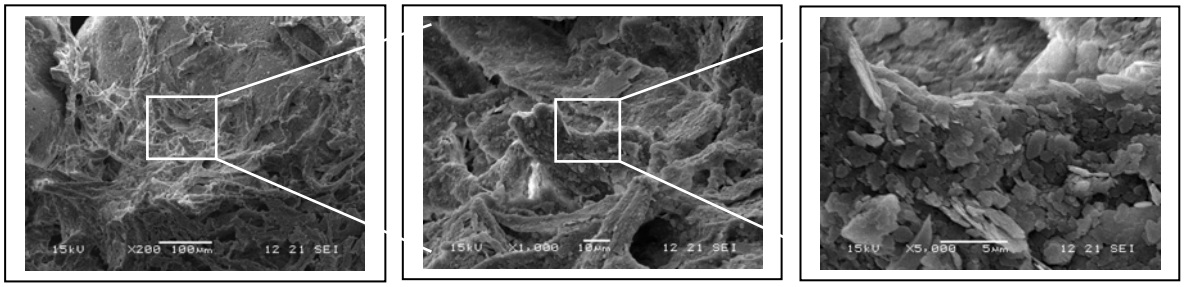

Figure 8. Secondary electron images of the BW40/kaolin/sand poultice seen in three different scales.

These two poultices have a pore size distribution partially overlapping that of the substrate, the pores are open, and a good desalination efficiency is remarked. The poultice BW40/kaolin/sand having the best pores connectivity, (MIP shows that all range of pores are interconnected, see Figure 6) presents the best efficiency.

The bentonite/sand poultice shows large pores centred on 90 µm, as determined by mercury porosimetry (see Figure 6). This porosity may still correspond to a part of the intergranular spaces between sand grains (0.5-1 mm). Larger pores, above 200 µm are also observed on SEM images (see Figure 9). Nevertheless, two other types of pores can be observed by SEM: one around 10 µm corresponding to the shrinkage cracks between the bentonite binder and sand grains, and a second one related to the microporosity of the bentonite binder itself. Batches of bentonite are all oriented; a real network of dense clay minerals is divided by a pore plate-like porosity of 1 µm. Indeed, pore geometry in porous material is complex and different geometries can be distinguished. In stone for instance, the nodal pores are supposed to be spherical, the sheet-like throats supposedly flat and the tube-like throats with a circular cross-section (Bernabe, 1991). A similar vocabulary is used here to describe the poultice structure. Such porosity might be poorly accessible, as it has been not detected by mercury intrusion.

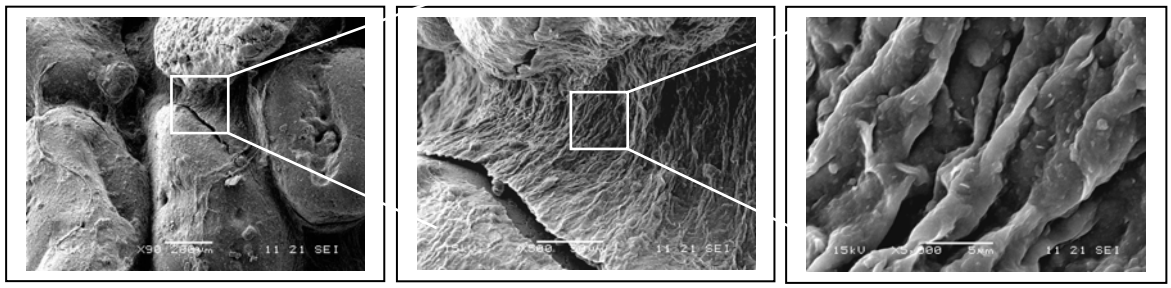

Figure 9. Secondary electron images of the bentonite/sand poultice seen in three different scales.

The porous network of the fine sand/fume silica poultice could only be identified by SEM, because the poultice is too fragile to be analyzed by mercury porosimetry. As can be seen on Figure 10, the fume silica forms crackled coatings and bridges all around and in between the sand grains. The largest cracks are around 10 µm, while the finest are of 1 µm, and both form a real sheet-like throat pore network. The large

cracks of the fume silica coating are probably the cause of the poultice's weakness once it is dry.

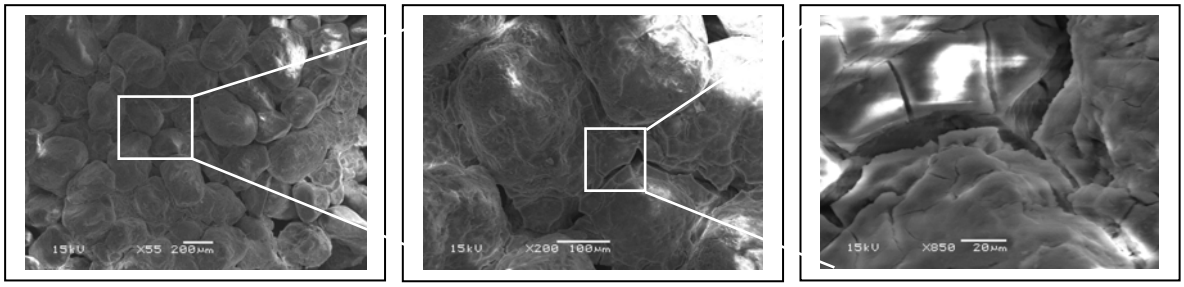

Figure 10. Secondary electron images of the fine sand and fume silica poultice at three different scales.

In our opinion, bentonite/sand and fine sand/fume silica poultices show a poor efficiency, because although they have fine pores, these are not able to induce a proper suction from the microporous substrate. The orientation and shape of pores seem to have an influence on the suction properties. Indeed, capillary suction of sheet-like throats is necessarily less effective than pores with tube-like throats – the capillary suction being due to an assumed radius and not from a wall to wall distance [Gregg and Sing, 1982].

Finally, cellulose poultice shows a unimodal pore size distribution centred on 10 µm (see Figure 6). Such a macrostructure is confirmed by SEM images, where a real snarl of fibres of different lengths and shapes can be observed (see Figure 11). The pore network is unfastened and unsorted. As fibres are not oriented, pore shape cannot be considered to be sheet-like throats, but are closer to a tube-like throats model. Nevertheless, the pores are way too large to exert suction on St Philibert stone – no efficiency is noticed.

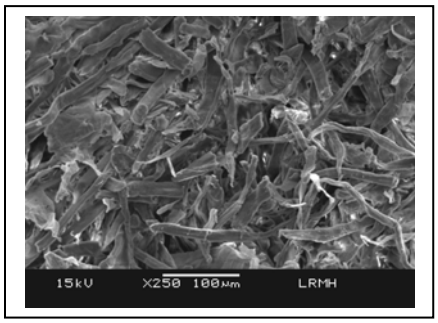

Figure 11. SEM images of the BW40/BC1000 poultice at three different scales.

3. Conclusion

This study perfectly illustrates the necessity for pore size distribution of both substrate and poultice to overlap one another in order to obtain a good salt extraction. In this specific case and in the environmental conditions considered (T°12C and 70% RH), kaolin/sand and BW40/kaolin/sand poultices showed the best salt extraction results.

Our analyses also suggest that an even pore size distribution, may lead to an optimization of desalination efficiency. Thus, size and arrangement of grains are probably important parameters to take into consideration when formulating poultices. As a matter of fact, they influence the connectivity between pore classes, as illustrated by the better performance of BW40/kaolin/sand poultice when compared to the kaolin/sand poultice. Pore shape may also have a significant influence on suction properties. Sheet-like throats seem less effective than tube-like throats. Finally, pure cellulose poultices introduce such high quantities of water that it cannot be absorbed back into the poultice. In our case, this has led to an increase of soluble salt content, and resulted in a concentration very close to the surface.

In conclusion, water content, grain packing, pore size distribution and pore shape should be considered in addition to adhesion in order to optimize desalination systems.

Acknowledgements

The authors would like to thank Romain Elias, Ann-Flore Nisson for their substantial help in ion chromatography, Thomas Vieweger and his team who applied the poultices, Mr. Eric Pallot for his availability and Mikaël Guiavarc'h who helped in sample collection.

References

Bourgès A., Vergès-Belmin V. 2008. A new methodology to determine rheologic behavior and mechanical properties of desalination poultices. The 11th international congress on deterioration and conservation of stone, Torun, Poland, edition in process.

Bernabe Y., 1991, *Pore geometry and pressure dependence of the transport properties in sands*tones, Geophysics 56., No4, pp. 436-446.

Domaslowski W., Lewandowska M.K., Lukaszewicz J.W. 1998. *Badanie nad Konserwacja murow ceglanych* (Research on the conservation of brick masonries). Torun University Publishers.

Gregg S.J., Sing K.S.W. 1982. *Adsorption, Surface Area and Porosity.* second edition, Academic Press INC. 111-193.

NORMAL 13/83, 1983, Dosaggio dei Sali Solubili, CNR-ICR, Rome, Italy.

Terheiden K., Wienke K., Kaps C. 2002. Kompressenentsalzung – Einfluss des Kompressenmaterials auf den regenerativen Schadsalztransport, WTA-Colloquium Erhalten, Umnuzen, Ertüchtigen, Tagungsbeiträge, Aedificatio Verlag Freiburg, 285-293.

Vergès-Belmin V., Siedel H. 2005. Desalination of Masonries and Monumental Sculptures by Poulticing: a Review. *Restoration of Buildings and Monuments* **11**, 6, 391-408.